



On the impact of co-feeding aromatics and olefins for the methanol-to-olefins reaction on HZSM-5



Xianyong Sun, Sebastian Mueller, Hui Shi, Gary L. Haller, Maricruz Sanchez-Sanchez, Andre C. van Veen, Johannes A. Lercher^{*}

Department of Chemistry and Catalysis Research Center, Technische Universität München, Lichtenbergstrasse 4, D-85747 Garching, Germany

ARTICLE INFO

Article history:

Received 20 December 2013

Revised 19 March 2014

Accepted 26 March 2014

Available online 19 April 2014

Keywords:

Methanol-to-olefins

Hydrocarbon pool

Selectivity

Co-feeding

ABSTRACT

The impact of adding various aromatic molecules (benzene, toluene, and xylenes) or olefins (ethene, propene, 1-butene, 1-pentene, and 1-hexene) to methanol over a HZSM-5 catalyst on activity and selectivity was systematically studied. Addition of a low concentration of aromatic molecules (16–32 C%), which are free of diffusion constraints, significantly enhanced the aromatics-based catalytic cycle and greatly suppressed the olefin-based cycle. This led to enhanced methane and ethene formation and methylation of aromatic rings at the expense of propene and C₄₊ higher olefins. The ratio of propene to ethene is controlled by the concentration of the aromatic molecules added. Co-feeding the same molar concentration of benzene, toluene and *p*-xylene influenced the methanol conversion to a nearly identical extent, as none of them experience transport constraints and the methylation rapidly equilibrates the aromatic molecules retained in the pores. In stark contrast, addition of small concentrations (10–40 C%) of C_{3–6} olefins with 100 C% methanol does not selectively suppress the catalytic cycle based on aromatic molecules. This led to unchanged selectivities to ethene and higher olefins (C₃₊). Within the C₃₊ fraction, the selectivity to propene decreased and the selectivity to butenes were enhanced with increasing concentration of the co-fed olefin. Because of the relatively fast rates in methylation and cracking of C_{3–6} olefins in the olefin-based cycle, the product distributions at high methanol conversion were identical when co-feeding C_{3–6} olefins with the same carbon concentrations. This work provides further insights into the two distinct catalytic cycles operating for the methanol conversion to produce ethene and propene over HZSM-5 catalysts.

© 2014 Elsevier Inc. All rights reserved.

1. Introduction

Methanol-to-hydrocarbon processes using microporous zeolites or zeo-type catalysts are regarded as a vital family of conversion technologies to bypass petroleum-based routes for the production of specific fuels and platform petrochemicals [1–6]. Methanol can be readily produced by proven technologies via synthesis gas, which in turn is generated by reforming carbon resources including coal, natural gas, and biomass. On the other hand, special significance of the methanol chemistry originates from its versatility of enabling selective transformations toward various products by proper choice of catalysts and reaction conditions [1–6]. Successfully implemented processes include Methanol-To-Gasoline [7,8], Methanol-To-Propene (both based on HZSM-5) [9–12], and Methanol-To-Olefins (based on SAPO-34, producing both ethene and propene) [13–15]. However, the typical single-pass selectivity

for many of these commercialized processes has remained limited since their inception, and substantial recycling is required.

Fundamental insights into the reaction mechanism play a vital role in achieving selectivity control. Ever since the first report by Chang and Silvestri [16], three decades of considerable experimental and computational research efforts have been dedicated to unraveling the complex reaction mechanism. Instead of the direct mechanisms, which involve the initial C–C bond formation directly from C₁ entities, the indirect “hydrocarbon pool” mechanism [17–19] is generally accepted for explaining the formation of light (C₂–C₄) olefins from methanol during steady-state operation. In the original “hydrocarbon pool” concept, the active site has been proposed to be located in the pores or cages of a microporous solid, comprised of an hydrocarbon species (organic part) and a proximate Brønsted acid site (inorganic part) [17–19]. It is described to act as a virtual scaffold for the assembly of light olefins and avoids unstable and high-energy intermediate species required for the direct C–C coupling mechanisms [17–23]. In a proposed cycle, methanol successively reacts with the hydrocarbon species via

^{*} Corresponding author. Fax: +49 89 28913544.

E-mail address: johannes.lercher@ch.tum.de (J.A. Lercher).

methylation, and subsequently elimination of light olefin products such as ethene and propene regenerates the initial hydrocarbon species [17–23].

Recent experimental and theoretical work demonstrated that focusing on polymethylbenzenes as the sole active species would cause a biased understanding on the MTO mechanism, and olefins may act as another kind of active “hydrocarbon pool” species in zeolites such as the medium-pore ZSM-5 zeolite with 3-D 10-ring channels, while aromatic intermediates seem to be kinetically-relevant for catalysts with large pores or voids [24,25]. This leads to the proposal and establishment of the “dual-cycle” mechanism [24,25], as shown in Scheme 1. Thus, considering that both aromatics and olefins exist in the zeolite pores, the corresponding olefin- and methylbenzene-mediated routes operate on a competing basis. Taking advantage of the different activities and selectivities of olefin- and aromatics-populated cycles toward ethene and propene formation, it has been hypothesized that one could optimize the product distribution through selectively propagating or suppressing one of the two (aromatics- and olefin-based) catalytic cycles.

Three potential strategies can be conceived for achieving selectivity control. Given that turnover of the aromatics-based cycle demands generally a larger space for the transition states than the olefin-based cycle, one approach is to adjust the pores by varying zeolite topologies [26,27]. Indeed, very recent experiments on methanol conversion over the one-dimensional 10-MR H-ZSM-22 zeolite without intersections showed that the sterically restricted topology suppressed selectively the reactions via the aromatics-based cycle and secondary aromatization via hydrogen transfer which would require larger transition states and reaction intermediates [28–31]. Thus, methanol conversion at 673 K proceeded exclusively via the olefin-based cycle, leading to a product mixture rich in C_{3+} branched alkenes, very low in ethene and almost negligible in aromatics [28–31]. The second strategy is to tune the inorganic part, i.e., the Brønsted acidity, through zeolite synthesis or post-synthetic anion or cation modifications, which have been documented in a large body of literature [2]. The third approach for selective propagation of a catalytic cycle is to influence the organic part, i.e., the concentration of olefin or aromatic species, by adding specific hydrocarbons together with methanol.

In this contribution, we explore this third approach by varying the nature and concentration of the co-processed hydrocarbons, to adjust the product selectivity under industrially relevant reaction conditions. Several reports on co-reacting hydrocarbons with methanol including various olefins and aromatics have appeared, but their main intentions were to elucidate the mechanistic features via isotopic labeling under conditions far away from realistic MTO(P) operations, and the impacts of co-feeding on product distributions is largely lacking [32–41]. Most recently, Ilias and Bhan reported in an elegant paper the impact on the product

distributions by co-processing low concentrations of toluene and/or propene with dimethylether, but the experiments were mainly performed at reaction temperatures as low as 548 K and a dimethyl ether pressure of 70 kPa [40]. To simulate industrial process conditions, experiments were performed with methanol pressure fixed at 10 kPa on a highly siliceous HZSM5 catalyst at 723 K. Various aromatic co-feeds including benzene, toluene and xylenes, and olefins including ethene, propene, 1-butene, 1-pentene, and 1-hexene were evaluated.

2. Experimental

2.1. Catalyst and reagents

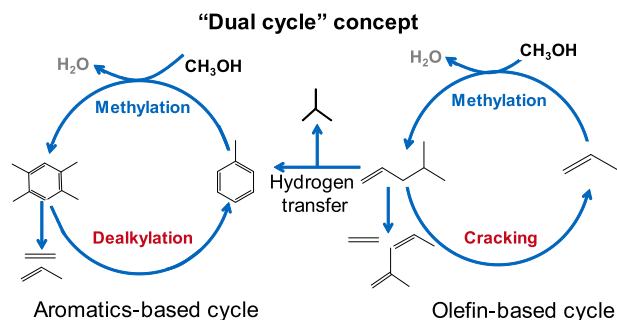
The specific synthesis method of the HZSM-5 (Si/Al = 90) was reported previously [42]. The as-synthesized material has a crystal size of 500 nm. The zeolite powder was pressed into a wafer, crushed, and sieved to a fraction of particle size in the range of 200–280 μm . Methanol (99.93%), 1-hexene, 1-heptene, benzene, toluene, *para*- and *meta*-xylenes (99.0%) were supplied by Sigma-Aldrich. Gases of C_{2-5} olefins (5% or 10% in volume diluted in N_2) were supplied by Westfalen GmbH.

2.2. Catalytic testing

All catalytic tests were performed on a bench-scale plug flow reaction unit. The catalyst pellets were homogeneously diluted with silicon carbide (ESK-SiC, 1:15 wt:wt) with a comparable particle size to ensure temperature uniformity. Catalysts were placed in a quartz tube (26 cm in length, 6.0 mm i.d.) and supported between two quartz wool plugs. The samples were activated at 753 K with the temperature control at the external surface of the quartz tube with 50 ml min^{-1} N_2 for 2 h prior to switching to feed. The reaction temperature was held at 723 K, and the total pressure was 108 kPa. The methanol partial pressure was maintained at 10 kPa. The total flow rate was held at 55 ml min^{-1} . Methanol vapor was fed by passing dry N_2 flow (29 ml min^{-1}) through the methanol-containing saturator which was thermo-stated at 298 K. Flow rates of gaseous olefin co-feeds (C_{2-5}) were controlled by mass flow controllers (Bronkhorst). For aromatics, 1-hexene or 1-heptene, the co-fed vapor was introduced by passing dry N_2 flow through a saturator containing the liquid reactant. Catalyst loading (2–100 mg) and reactant flow velocity were varied to achieve a wide range of contact time and methanol conversion. Here the contact time is defined as the ratio of catalyst mass to the molar flow rate of methanol. The reactor effluent was kept at 393 K and transferred via a heated line into a gas chromatograph (HP 5890) equipped with a HP PLOT-Q column (30 $\text{m} \times 0.32 \text{ mm} \times 0.5 \mu\text{m}$) connected to a flame ionization detector for on-line analysis. Product analysis was performed at steady-state conversions.

Both methanol and dimethyl ether were treated as reactants. The concentration of a co-feed is given as a molar ratio of its partial pressure to methanol partial pressure (10 kPa). The product distributions (concentration and yield) were given on a carbon basis, and the carbon in the methanol feed with a partial pressure of 10 kPa was defined as 100%. For instance, a feed of 0.4 kPa toluene and 10 kPa methanol is depicted as co-feeding 4 mol.% toluene. As one toluene molecule has seven carbon atoms, 28% toluene with 100% methanol in carbon, the feed was referred to as containing a total carbon concentration of 128% (28 C% from toluene with 100 C% from methanol) in the feed.

In the experiments of methanol conversion with aromatic co-feeds, the final aromatics increment after reaction is defined as the aromatics concentration (in C%) from which the initial concentration of the aromatics co-feed (in C%) is subtracted.



Scheme 1. Proposed “dual-cycle” mechanism in methanol-to-olefins conversion over HZSM-5 [24,25].

3. Results and discussion

3.1. Reaction pathway of methanol-to-olefins conversion over HZSM-5 catalysts

A detailed view on MTO conversion and product yields as a function of contact time over HZSM-5 at 723 K and methanol pressure of 10 kPa, is depicted in Fig. 1a. Methanol conversion leads to a wide variety of products including methane, ethene, propene, butenes, C₅ hydrocarbons, C₆₊ aliphatics, other light paraffins (C_{2–4}), and aromatics. Hereby, the C₅ fraction designates all hydrocarbons with five carbon atoms, and the C₆₊ aliphatics includes all other heavier hydrocarbons other than aromatics. Light paraffins include methane, ethane, propane, n-butane and isobutane, while aromatics include benzene, toluene, xylenes, trimethylbenzenes, and tetramethylbenzenes. Hydrogen transfer (HT) products include aromatics and C_{2–4} light paraffins. In the absence of an added reactant, the effect of contact time on methanol conversion is characterized by an initiation phase preceding the on-set of methanol conversion. At the initiation phase, methanol is dehydrated to dimethyl ether (DME) until thermodynamic equilibrium is established. Only when a certain amount of hydrocarbon species had been built up, the methanol conversion started up at a critical contact time (0.03 min kg_{cat} mol^{−1}_{MeOH}). The methanol conversion showed a self-acceleration and was complete within a narrow range of contact times. The typical S-shaped curve, characteristic of an autocatalytic phenomenon, indicates that some of the products provide new reaction routes of methanol conversion [43].

The concentrations of propene and C₅ hydrocarbons reached a maximum approximately at the contact time when methanol conversion attained 100%, followed by a slight decline with increasing contact times (Fig. 1a). Ethene, light paraffins (C_{1–4}), and aromatics were formed with low concentrations (ca. 8 C% in total), all increasing with contact time. This is generally in line with the simplified pathway shown on Scheme 2.

However, two product groups, C₆₊ aliphatics and ethene, deserve further attention. The concentrations of C₆₊ aliphatics peaked when the methanol conversion was ca. 80%, then decreased with further increasing methanol conversion and finally leveled off at even longer contact times (Fig. 1a). Considering that methanol inhibits olefin adsorption, even in low concentrations (e.g., until only 20% remaining) [41], we attribute the formation of C₆₊, particularly at lower contact times, mainly to the methylation of C_{3–5} olefins, and not to olefin oligomerization. Noted that there was only a slight increase in the yields of hydrogen transfer products with longer contact time, it is concluded that further conversion of these higher olefins is mainly due to the formation of C_{3–5} light olefins by cracking rather than ring closure and aromatization. This behavior indicates that olefin methylation to higher olefins (mainly C₆ and C₇) and cracking of these higher olefins are two critically important steps in the reaction network, and C₆₊ olefins act as reaction intermediates [44,45]. Very different from C₃₊ olefins, ethene formation followed a similar trend to that of aromatics with increasing contact time (Fig. 1a), suggesting that ethene formation has a mechanistic relationship with the formation of aromatic molecules [25]. These observations are generally in line with the current dual-cycle mechanism over HZSM-5.

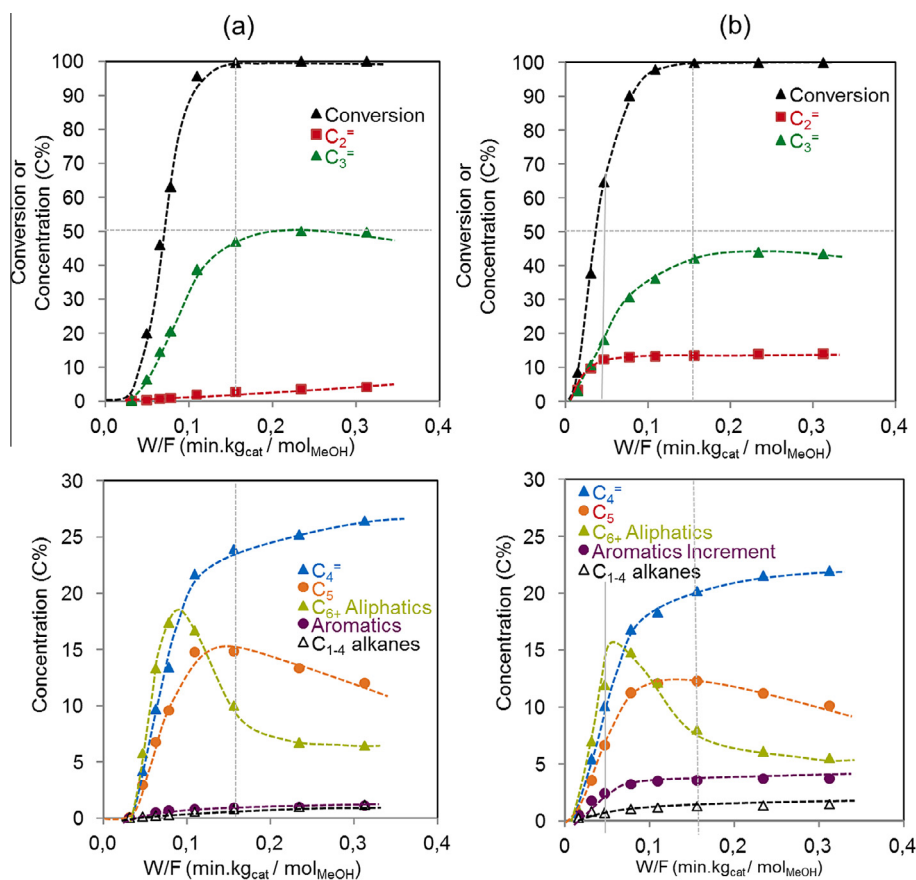
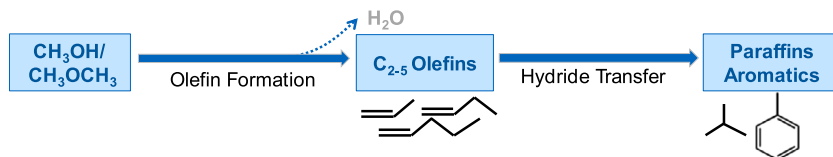


Fig. 1. Conversion/concentration profiles as a function of contact time for feeds of pure methanol (a) and methanol with 4 mol.% *p*-xylene (b) over HZSM-5 catalyst at 723 K. Product concentrations were calculated on the carbon-number basis through defining the carbon concentration in methanol as 100 C%. Hereby the aromatics increment was calculated by subtracting the product concentration (in C%) by 32 C% (the initial carbon in 4 mol.% *p*-xylene which contained eight carbon atoms).



Scheme 2. A simplified reaction pathway of methanol conversion over HZSM-5 catalysts.

3.2. Impact of aromatics co-feeding on the methanol conversion

To investigate the influence of specific aromatic co-feeds on the methanol conversion, experiments were performed with several aromatic molecules at 723 K and a methanol partial pressure of 10 kPa. The aim was to explore whether co-feeding a low concentration of aromatic molecules would selectively propagate the aromatics-based cycle and if so, to study the effect of co-feeding aromatics on modulating the product distribution. First, the impact of co-feeding different concentrations (molar ratios of aromatics to methanol being 2 or 4 to 100% methanol) of *p*-xylene is shown, followed by comparison with that of co-feeding *m*-xylene. Then, the effect of co-feeding lower substituted aromatics, toluene and benzene, was examined.

3.2.1. Impact of co-feeding *p*- or *m*-xylene

Co-processing of methanol with xylenes was carried out at reaction conditions similar to the experiments in the absence of co-feed. The feed was composed of methanol and *p*-xylene in a molar ratio of 50 or 25 (2 or 4 mol.% of *p*-xylene). In contrast to most previous reports [41,38,46], low molar ratios of co-feeds to methanol were used in this study for several reasons, i.e., (i) to mimic the realistic on-site conditions of a MTP operation; (ii) to avoid methylation of aromatics rather than methanol conversion as the main catalytic reaction; and (iii) to keep the initial catalyst surface covered mainly by methanol or intermediates derived from it rather than by the co-fed aromatics.

The initiation phase for methanol conversion was dramatically shortened when *p*-xylene (2 mol.%) was co-fed. However, the S-shaped curve still remained. Further increase in *p*-xylene concentration from 2 to 4 mol.% led to insignificant enhancement in methanol conversion at any contact time (Fig. 2). If aromatic species would act as classic components in autocatalysis kinetics, higher concentrations of an intermediate product should result in progressively higher conversion rates. Thus, we conclude that *p*-xylene cannot be the main product responsible for autocatalysis under the conditions of these experiments.

The effect of contact time on the product concentrations, with a mixed feed of methanol and *p*-xylene in a molar ratio of 25, is shown in Fig. 1b. At methanol conversion of 8.4%, the main products were ethene and propene, the selectivity being 39% and 36%, respectively, and the other products were mainly butene isomers (10%) and C_{5-7} olefins (4% and 6% each). At higher methanol conversions, the propene concentration drastically increased and surpassed that of ethene by a factor of ca. 3 at the highest contact time. As shown in Fig. 1b, while ethene concentration nearly leveled off at a methanol conversion of 70%, the propene concentration continued to increase. Concurrently, butenes and C_{5-7} olefins evolved in a manner similar to that observed with pure methanol. During the increase in methanol conversion from 70% to 100%, 30% carbon in methanol, together with 10% carbon in C_{6-7} aliphatics, was converted to C_{3-5} olefins (Fig. 1b). This indicates that although the aromatics-based cycle contributes significantly to methanol conversion and ethene formation, the olefin-based cycle, which contributes to the formation of propene and higher olefins, is not completely suppressed by co-feeding *p*-xylene.

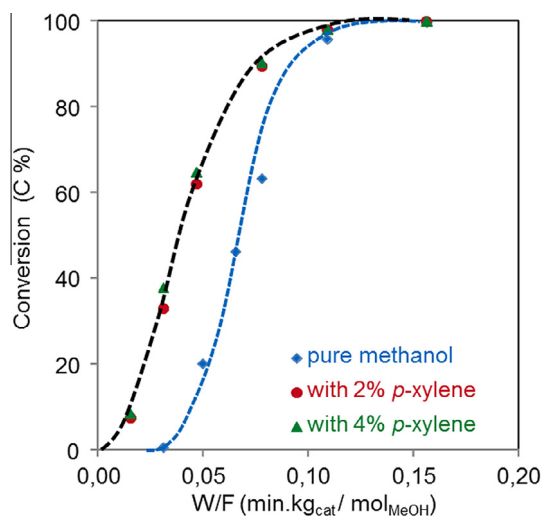


Fig. 2. Impact of *p*-xylene co-feeding on methanol conversion as a function of contact time. Methanol pressure was 10 kPa and reaction temperature was 723 K. The partial pressure of *p*-xylene was 0, 0.2, 0.4 kPa, leading to a ratio of *p*-xylene to methanol being 0, 2 or 4 to 100 (0%, 2% or 4%).

The yields of ethene, aromatics and methane increased, while those of propene and higher olefins decreased, with increasing concentration of *p*-xylene in the feed (Fig. 3). In particular, the yields of ethene and aromatics increased by ca. 4 times, from 3.5 to 14 C% and from 0.8 to 3.6 C%, respectively, when the feed changed from pure methanol to 4 mol.% *p*-xylene-containing methanol.

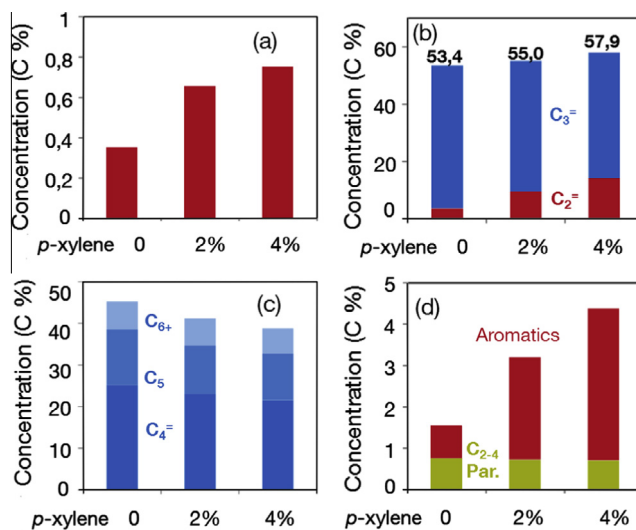


Fig. 3. Influence of the *p*-xylene addition on the product distribution in terms of methane (a), ethene and propene (b), C_4 , C_5 , and C_{6+} aliphatics (c), C_{2-4} paraffins and aromatics increment (d) at a contact time of 0.23 min.kg_{cat}/mol_{MeOH}. Reaction temperature was 723 K, methanol partial pressure 10 kPa and partial pressures for *p*-xylenes 0, 0.2 or 0.4 kPa.

These observations, along with the high fractions of trimethylbenzenes and tetramethylbenzenes in aromatics (Fig. S1), demonstrated that co-feeding *p*-xylene propagates the aromatics-based cycle via aromatics methylation and elimination of methane and light olefins (predominantly ethene and propene). On the other hand, the olefin-based cycle was suppressed when *p*-xylene was co-fed, as shown by the lower yields of propene and C_{4–7} olefins.

The total yield of ethene and propene slightly increased with increasing *p*-xylene concentration in the feed (Fig. 3b). Therefore, by varying the concentration of co-fed *p*-xylene, the ratio of propene to ethene can be varied without loss of selectivity to total light olefins, and both propene-targeted and light-olefins-targeted production can be realized without changing the reaction temperature and methanol pressure. As depicted in Fig. 4a, the yields of C_{2–4} paraffins, formed via hydrogen transfer reactions of olefins, were comparable between pure methanol and feeds containing *p*-xylene.

In a typical hydrogen transfer reaction, the paraffin and aromatics molecules are produced with a stoichiometric ratio of three to one during hydrogen transfer between olefins (Scheme 3, route 1). As a result, aromatics produced from such routes should have been observed with at most one third of the yield of C_{2–4} paraffins. As the actual fraction of aromatics formed was significantly higher than C_{2–4} paraffin yield when co-feeding *p*-xylene (Fig. 4b), the aromatics surplus must come from the incorporation of carbon in methylating C₁ species derived from methanol (Scheme 3, route 2). This interpretation is further supported by the detailed analysis on the carbon distribution in aromatics increment, shown in Fig. S2. While the fraction of carbon in the aromatic ring (Fig. S2a) is comparable for the feeds with *p*-xylene co-fed or with pure methanol, co-feeding *p*-xylene enhances the aromatics methylation, leading to the significantly increased carbon concentration in the side chains.

When *m*-xylene was used as the co-feed with a methanol-to-xylene molar ratio of 25, the critical contact time after which

methanol conversion became detectable was shortened by about 50% (Fig. 5a). Compared to the values observed for pure methanol feed, ethene yield was promoted from 3.5 to 5.1 C%, while the propene yield decreases slightly from 49.9 to 49.0 C% when 4 mol.% *m*-xylene was co-fed (Fig. 5c). These effects were much less significant compared to those imposed by co-feeding of *p*-xylene.

The main reason is attributed to steric constraints. The dimension of the pore size of MFI zeolite is about 0.6 nm, while the molecular size for *p*- and *m*-xylene is 0.58 and 0.68 nm, respectively. The diffusion rate for *m*-xylene to access the zeolite Brønsted acid sites is lower than that of *p*-xylene. Therefore, the enhancement by *m*-xylene on the aromatics-based cycle is less prominent than that of *p*-xylene. This is also in line with the increment of aromatics concentration (Fig. 5d). The aromatics increment (2 C%) in the feed containing *m*-xylene was significantly lower than the increase (3.1 C%) with the feed containing *p*-xylene, indicating that *m*-xylene faced diffusional constraints and constraints of being methylated, a pre-requisite for the aromatics-based cycle to initiate and turnover.

3.2.2. Impact of toluene and benzene co-feeding on methanol conversion

Having shown that the aromatics-based cycle operates over HZSM-5 and can be selectively propagated through co-feeding low concentrations of xylenes and that the olefin-based cycle can be suppressed, the question arises how other aromatic molecules, such as toluene and benzene, influence activity and selectivity.

At a molar methanol-to-aromatics of 25, methanol conversion changed with increasing contact time in a manner independent of the nature of co-fed aromatics (Fig. 6). After full methanol conversion was reached, ethene and propene yields from a toluene-containing feed were slightly lower than those from a reactant stream containing *p*-xylene. Co-feeding with benzene led to even lower yields to ethene and propene, i.e., 12.8% and 40.4%,

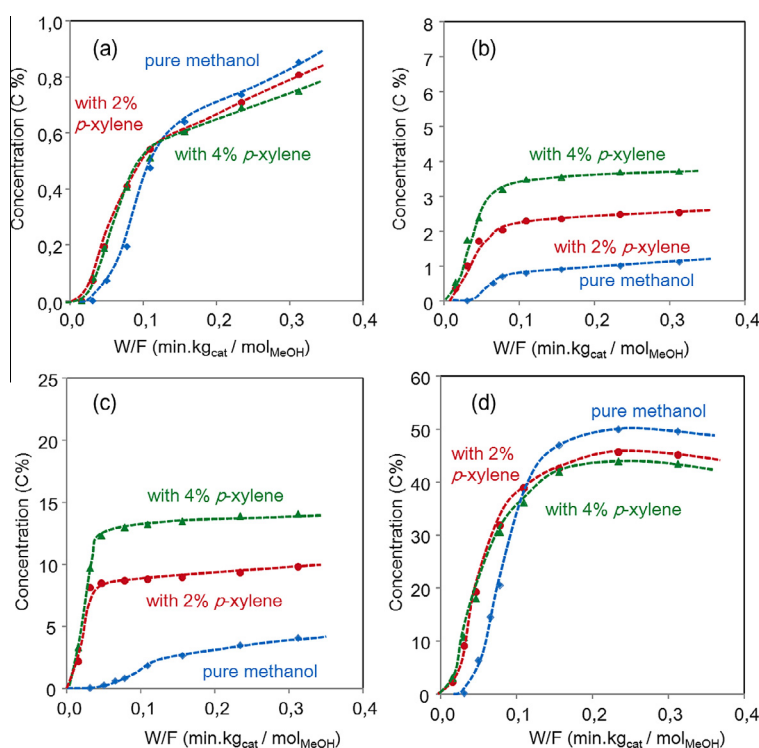
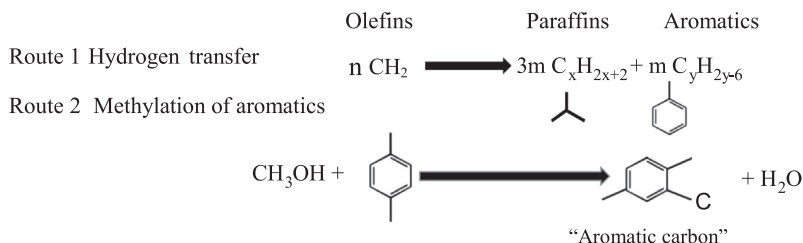


Fig. 4. Impact of co-feeding different concentrations (2 or 4 mol.%) of *p*-xylene on the yield of C_{2–4} paraffins (a), aromatics increment (b), ethene (c) and propene (d). Reaction temperature was 723 K, methanol partial pressure 10 kPa and partial pressures for xylenes 0, 0.2 or 0.4 kPa.



Scheme 3. Two representative routes for aromatics increment.

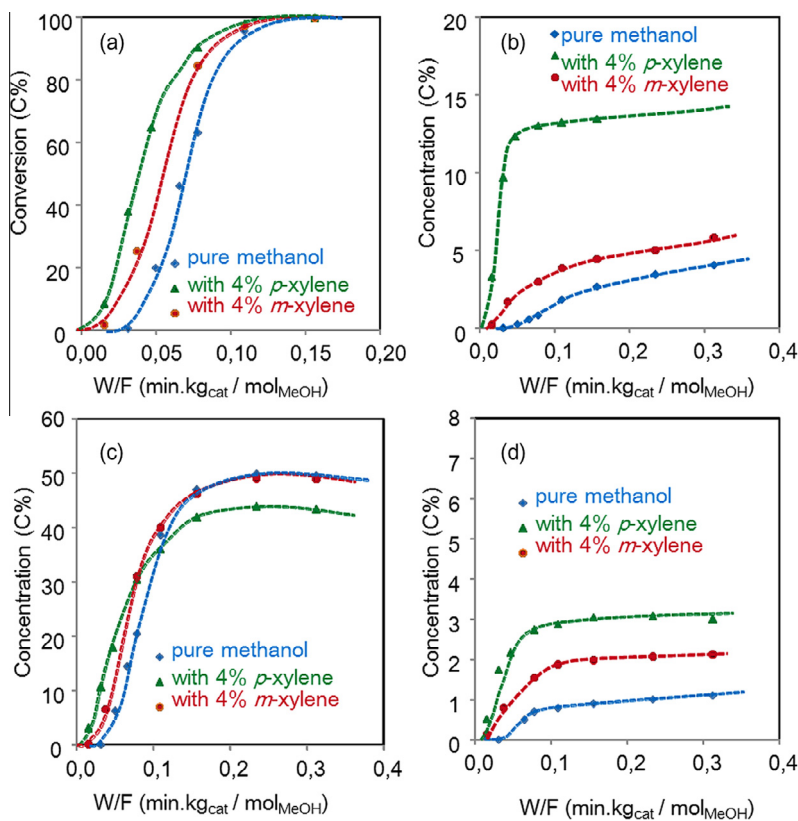


Fig. 5. Impact of *m*-xylene co-feeding on methanol conversion (a), ethene yield (b), propene yield (c) and aromatics increment (d). Pure methanol feed and *p*-xylene co-feeding were included as references. Reaction temperature was 723 K, methanol partial pressure 10 kPa and partial pressures for xylenes 0.4 kPa.

respectively. Compared to the feed containing *p*-xylene, the toluene-containing feed gave rise to significantly larger increase in the aromatic products (6.0 C% vs. 3.1 C%), while yielding a comparable amount of C_{2–4} light paraffins. This is attributed to a higher degree of methylation of toluene than of *p*-xylene. In turn, the aromatics increment when co-feeding benzene was ca. 4% higher than that from toluene, indicating that all the co-fed 4% benzene was methylated. As more methanol was consumed in methylation of the aromatic ring with benzene and toluene than with *p*-xylene, a slightly lower concentration of ethene and propene was observed than with *p*-xylene. A similar trend was also observed from comparison of the impact of co-feeding 2 mol.% benzene, toluene, and *p*-xylene, as shown in Fig. S3.

In consequence, we conclude that the relative selectivity to ethene and propene can be modulated by recycling a suitable fraction of aromatics products. As co-feeding of benzene, toluene and xylenes essentially influences the methanol conversion in an identical way, only the ratio between the aromatic molecules and methanol controls this selectivity.

3.3. Impact of co-feeding olefins on methanol conversion

Analogous to the experiments carried out with various aromatics, the impact of co-feeding a specific olefin on methanol conversion has been investigated. Experiments were performed with various olefins at 723 K and methanol partial pressure of 10 kPa. The aim was to study whether co-feeding a certain concentration of olefins could selectively propagate the olefin-based cycle and could impact the product distribution. First, the impact of co-feeding different concentrations of 1-pentene (molar ratios of methanol-to-olefin were 50, 25 and 12.5) was shown, followed by comparison of the impact of the size of the alkene (ethene, propene, 1-butene, 1-hexene).

3.3.1. Impact of 1-pentene co-feeding on the methanol conversion

Co-feeding olefins is another conceived potential strategy for tuning product selectivities. 1-pentene was co-fed with methanol in a molar methanol-to-1-pentene ratio of 50, 25 and 12.5. In analogy with the addition of aromatics, co-feeding 1-pentene led to a

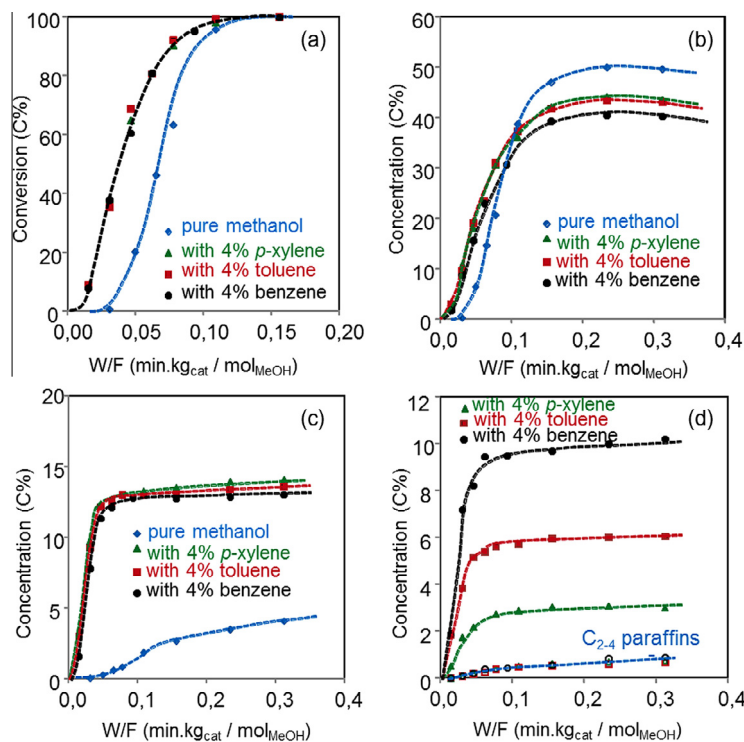


Fig. 6. Impact of co-feeding 4 mol.% toluene or benzene on methanol conversion (a), propene yield (b), ethene yield (c), the yield of C₂₋₄ paraffins (d, open symbols), and concentration increment of aromatics (d, closed symbols). Pure methanol and 4% *p*-xylene were shown as references.

shorter initiation phase (Fig. 7). In stark contrast to the case of aromatics co-feeding, however, further increase in 1-pentene concentration from 10 to 40 C% in the feed led to higher rates. Therefore, we conclude that olefins, rather than aromatic molecules act as the crucial species enhancing the conversion rate. The S-shaped curve characteristic of autocatalysis was observed with 8% co-fed 1-pentene. It is interesting to note that at very high concentrations of olefin addition (a ratio of one on a molar basis), methanol conversion followed a pseudo first-order kinetics instead of a sigmoid curve [41]. Under the conditions of this latter study, methanol tends to be converted via methylation of the co-fed pentene, when the molar concentration of olefin is at least comparable to the methanol concentration. In this case, the conversion of methanol followed a first-order rate law, because methylation of 1-pentene

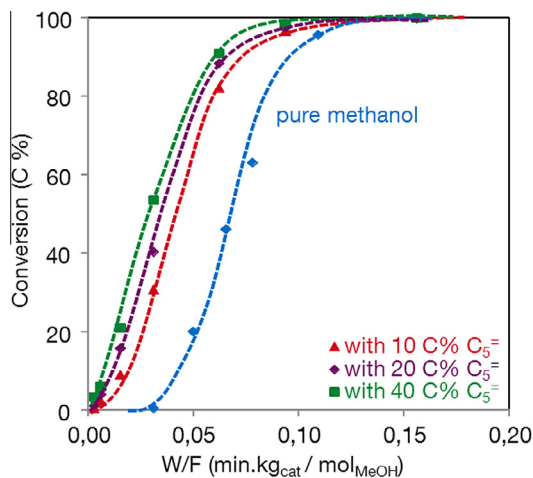


Fig. 7. Impact of the concentration of co-fed 1-pentene on the methanol conversion. Reaction temperature was 723 K, methanol partial pressure 10 kPa, 1-pentene partial pressure 0.2, 0.4, 0.8 kPa, respectively.

had higher rate constant than the methylation of any other lower olefins [41]. When only a low concentration of pentene was co-fed with methanol, most methanol molecules would undergo autocatalytic MTO reaction, rather than direct methylation of the co-fed pentene [4].

Fig. 8 depicts the evolution of product concentrations with increasing contact time for the feed containing 1-pentene (20 C%). At the shortest contact time, 1-pentene (and likely its isomers) underwent a rapid methylation, evidenced by the rapid increase in the concentration of C₆₊. The product distribution at the shortest contact time studied is listed in Table 1. From these

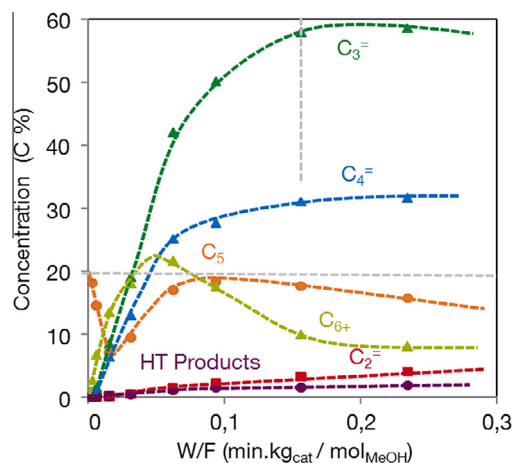


Fig. 8. Concentration of various hydrocarbons as a function of contact time for the feed of methanol with 20 C% from 1-pentene. Reaction temperature was 723 K, methanol partial pressure 10 kPa, 1-pentene co-feed partial pressure 0.4 kPa. The horizontal dashed line indicated the concentration of initial 20 C% from 1-pentene. The vertical dashed line indicated the contact time at which the 100% conversion of methanol was reached.

Table 1

Conversions and product distributions at low contact times, i.e., <0.01 (min kg_{cat} mol_{MeOH}⁻¹). Reaction temperature was 723 K, methanol partial pressure 10 kPa, co-feeding 20 C% from propene, 1-butene, 1-pentene or 1-hexene. The flow rate was kept identical at 55 ml min⁻¹.

Co-feed (20 C%)	Catalyst amount (mg)	Methanol conversion ^a	Hydrocarbons (C%)							HT products
			C ₁	C ₂ ⁼	C ₃ ⁼	C ₄ ⁼	C ₅	C ₆	C ₇ +	
C ₃ ⁼	2.5	1.9	0.04	0.01	17.4	2.52	0.82	0.63	0.45	
1-C ₄ ⁼	2.5	4.1	0.06	0.04	1.38	14.4	4.16	2.89	1.09	0.05
1-C ₅ ⁼	1	1.5	0.04	0.02	0.37	0.32	17.8	2.22	0.43	
1-C ₆ ⁼	5	13.9	0.09	0.21	8.80	6.69	4.56	8.29	0.93	0.17

^a The lowest conversion for each co-feeding experiment.

experiments, we derive that at differential conditions, the conversion rate of methanol was estimated to be twice the rate of pentene disappearance. This suggests that pentenes are not all methylated by methanol in a 1:1 ratio, and that multiple methylation events of pentenes to heptenes likely occur. Alternatively, this can be ascribed to the fact that a part of the methanol is not consumed in methylating pentenes; this fraction converts to olefins, as evidenced by the formation of C_{2–4} olefins at such a short contact time (Table 1).

After a certain contact time, the pentene concentration started to increase, and the following trend for each group was similar to that observed for the conversion of methanol alone (Fig. 1a), indicating that co-feeding 1-pentene does not alter the dominant reaction pathway. At a certain contact time, the yield of a specific product or group of products, e.g., propene, from methanol with

co-fed pentene was higher than that from pure methanol (Fig. 8 compared with Fig. 1a), as 1-pentene was fully converted via methylation and cracking.

Fig. 9 shows the comparison of the product distribution for the feeds without or with various concentrations of 1-pentene co-feed at the same methanol contact time of 0.23 min kg_{cat} mol_{MeOH}⁻¹. In stark contrast to the addition of aromatic molecules, co-feeding 10–40 C% 1-pentene significantly reduced the formation of methane, which is concluded to have formed mainly via demethylation of polymethylaromatics. For pure methanol or methanol with aromatics, the initial phase of the methanol reaction is dominated by the aromatics-based cycle, leading to methane formation. In the presence of pentene, the olefin-based cycle dominates the conversion pathway, in which β -scission necessarily leads to insignificant rates of methane formation. On the other hand, co-feeding

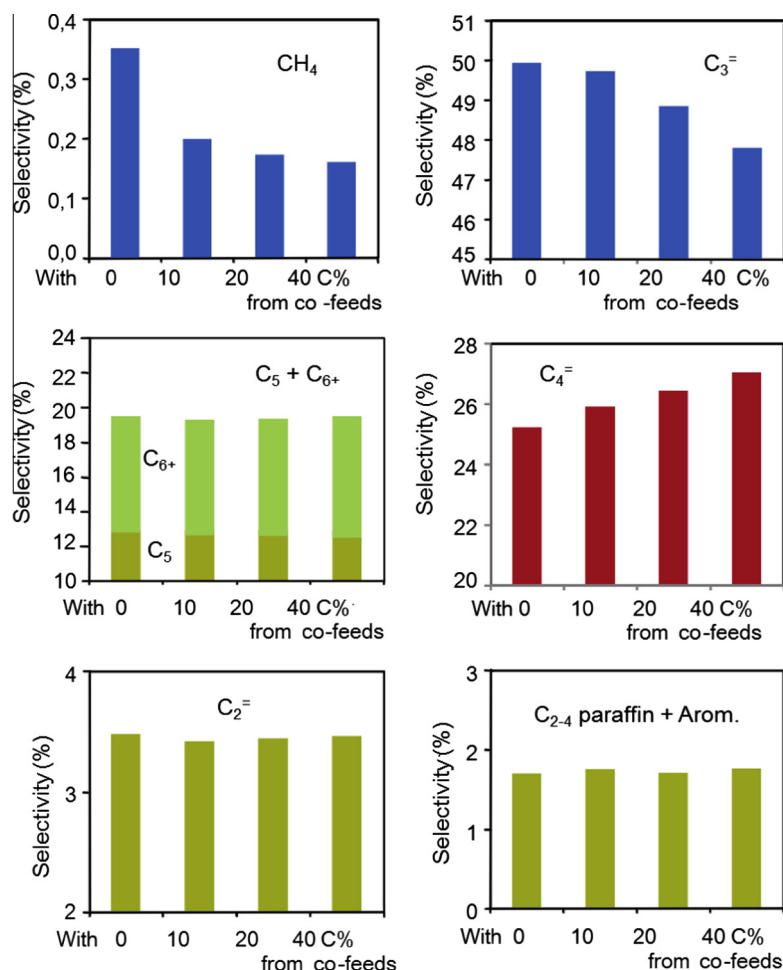


Fig. 9. Influence of the concentration of co-fed 1-pentene on the total product distribution. Reaction temperature was 723 K, methanol partial pressure 10 kPa, 1-pentene co-feed partial pressure 0.2, 0.4, 0.8 kPa, respectively, contact time 0.23 min kg_{cat} mol_{MeOH}⁻¹.

1-pentene showed little impact on the selectivities to ethene and C_{2-4} paraffins resulting from hydrogen transfer. In marked contrast to the case of co-feeding aromatic molecules, the addition of low concentrations of 1-pentene neither suppressed the aromatics-based cycle nor promoted significantly the olefin-based cycle. The main consequence of co-feeding 1-pentene was the decrease in the selectivity to propene and the increase in the selectivity to butenes (Fig. 9).

This impact can also be demonstrated with Fig. S4. Compared to the pure methanol feed, the feed with 10 C% from 1-pentene produced 0.3 C% more ethene, 5.1 C% more propene and 3.4 C% more butenes (in total 8.8 C% to C_{2-4} olefins). On the other hand, the yield of C_5 fraction was 1.2 C% higher for the feed with 1-pentene. Considering that 10 C% was co-fed, the net impact is that 8.8% of the co-fed C_5 was transformed into C_{2-4} olefins, while the selectivities to other products from methanol conversion remained almost unchanged.

3.3.2. Impact of the nature of co-fed olefins on the methanol conversion

Fig. 10 shows the methanol conversion and product yields as a function of contact time for a methanol-olefin mixture, which contained 100% C from methanol and an equal amount of 20% C from one of the C_{3-6} 1-olefins, i.e., propene, 1-butene, 1-pentene, or 1-hexene. At methanol conversions below 50%, the nature of co-fed olefin impacted methanol conversion and product distribution. As methylation of the co-fed C_n olefins was the main reaction (Table 1), the C_{n+1} olefins were the main products except for the case of 1-hexene.

At methanol conversion higher than 70%, the product distribution no longer depended on the nature of the olefin co-feeds (Fig. 10). The methylation rate coefficients for C_{3+} olefins increase in order of carbon chain length [6]. Taking the propene co-feeding as an example, the propene molecules are methylated to form butenes, which have higher methylation reactivities than propene. This results in further methylation of butenes to pentenes, which

are in turn more active than butenes and propene in methylation and, thus, have a high tendency to be methylated further to hexenes. At the prevalent reaction conditions, hexenes are much more reactive than butenes and pentenes in cracking. In consequence only some hexene desorbed as product, some molecules were cracked to propene, and some further methylated to heptene, which either desorbs (minor) as product or undergoes cracking (major) to form propene and butenes. Cracking of hexenes and heptenes was relatively fast. Therefore, the carbon chain growth practically terminated at heptenes.

The fast methylation and cracking of C_{3+} higher olefins results in extensive scrambling of the co-fed carbon and, thus, the final product distribution is dominated by the concentration of added carbon, irrespective of the nature of the co-fed olefin. When C_{3+} olefins were co-fed with 40 C% concentration with respect to methanol (100 C%), the product distribution also remained unchanged at methanol conversions >60% for any C_{3-6} olefin fraction (Fig. S5). Accordingly, there is practically no need to co-feed a specific olefin fraction, except for ethene (vide infra). As shown in Figs. 8, S5 and 10, the yield of propene was improved, e.g., from 50% to 60%, by co-feeding C_{3-6} olefin with methanol, but the total C-based selectivity to propene was either indifferent or slightly lower by olefin co-feeding (Fig. 9).

Compared to the co-feeding of C_{3-6} olefins, co-feeding ethene led to a different impact on methanol conversion with increasing contact time (Fig. 11). The reactivity of ethene in methylation has been reported to be at least one order of magnitude lower than the C_{3+} olefins. The low activity of ethene has led, therefore, to a slower conversion of methanol compared to the addition of other higher olefins. It also indicates a slow incorporation and scrambling of the carbon of ethene into the other higher products.

The fact that the product distribution was independent from the nature of olefin added is a further evidence that the olefin-based cycle is the dominant reaction pathway over HZSM-5 under the studied reaction conditions (at higher conversion of methanol). However, addition of olefins favors hydrogen transfer and the

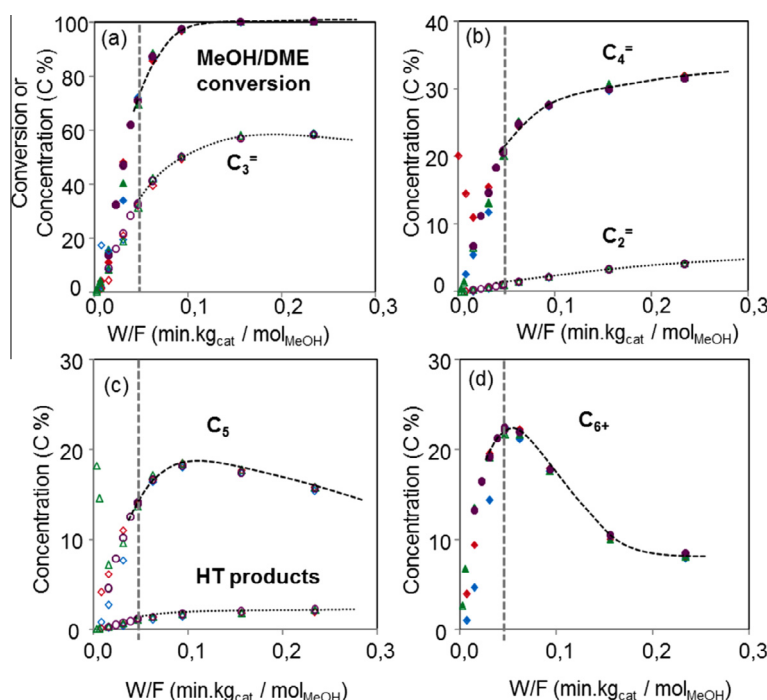


Fig. 10. Reaction path for the conversion of 100% methanol with 20% carbon from propene (blue), 1-butene (red), 1-pentene (green), 1-hexene (purple), in terms of conversion and propene (a), butenes and ethene (b), C_5 and HT products (c), and C_{6+} (d). Reaction temperature was 723 K, methanol partial pressure 10 kPa. Partial pressures for propene, 1-butene, 1-pentene or 1-hexene were 0.67, 0.5, 0.4, 0.33 kPa, respectively, leading to an equivalent 20% co-fed carbon in each feed mixture. (For interpretation of the references to color in this figure legend, the reader is referred to the web version of this article.)

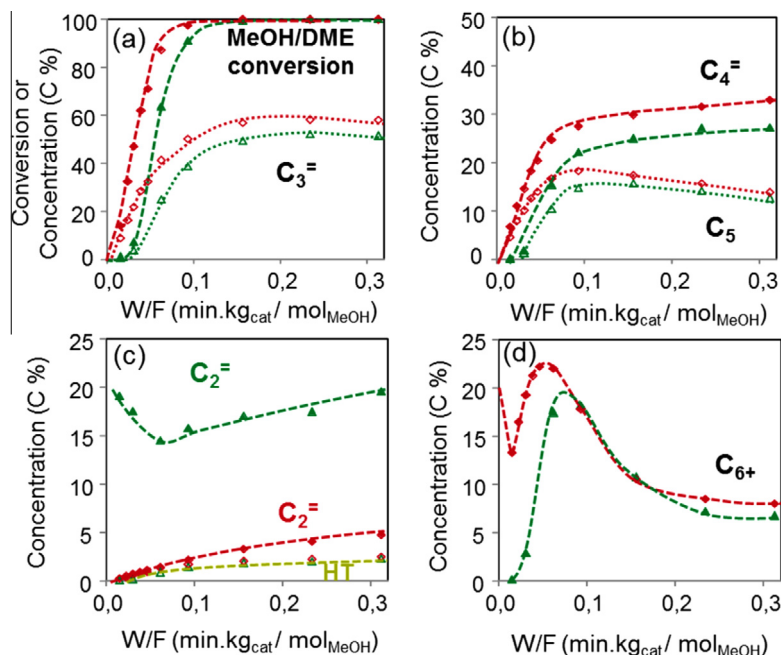


Fig. 11. Comparison of reaction path for 100% methanol with 20% carbon from ethene (green) and 1-hexene (red), in terms of methanol conversion and propene (a), butenes and C₅ (b), ethene and HT products (c), and C₆+ (d). Reaction temperature was 723 K. Methanol partial pressure was 10 kPa, and partial pressures for ethene and 1-hexene were 1 and 0.33 kPa, respectively, leading to the equivalent 20 C% in each feed mixture. (For interpretation of the references to color in this figure legend, the reader is referred to the web version of this article.)

formation of aromatics. In turn, the aromatic molecules based route remains active, as shown by the methanol conversion rates in Section 3.3.1. The overall consequence is, therefore, that co-feeding olefins does not selectively propagate the olefin-based cycle. In other words, the ratio of activities of aromatics and olefin-based cycles is not significantly changed by co-feeding small amount of olefins compared to the case of a pure methanol feed.

We note, however, that the results of impact of co-feeding olefins demonstrated in Fig. 9 is in marked contrast with the recent work by Ilias and Bhan [40], who report that co-processing propene significantly propagates the olefin-based cycle. In this case, results were reported at a reaction temperature of as low as 548 K and the comparison was made at a DME conversion of around 20% [40]. These conditions are highly different from the realistic industrial MTO(P) operations (reaction temperature higher than 723 K and methanol/DME conversion nearly 100%) [9–12] and the reaction conditions adopted in the present work. Under such lower reaction temperature and low methanol/DME conversion, methylation was much more favored than cracking. This led these authors to observe a remarkable increase in the selectivity of C₄–C₇ aliphatics when co-processing propene [40]. However, as showed in the present work, in a complete reaction pathway, these methylated higher olefins would undergo rapid cracking at higher methanol conversion facilitated by the usually higher reaction temperature. This essentially leads to the scrambling and re-distribution of the co-fed carbon, instead of selectively promoting the olefin-based cycle, as shown in Figs. 9 and S5.

4. Conclusions

Under reaction conditions close to those of the industrial MTP process operation, co-feeding a small concentration of aromatic molecules (16–32 C%), which are free of diffusion constraints, significantly propagates the aromatics-based catalytic cycle and greatly suppresses the olefin-based cycle, leading to higher

methane, ethene formation and aromatics methylation at the expense of propene and C₄+ higher olefins. The ratio of propene to ethene can be easily controlled by modulating the concentration of the aromatics co-feeds. Co-feeding the same molar concentration of benzene toluene and *p*-xylene influences the methanol conversion. The aromatic molecules with a lower degree of substitution become rapidly methylated to form the same active carbon species than xylenes.

In stark contrast, co-feeding small concentrations (10–40 C%) of C₃–C₆ olefins with 100 C% methanol does not selectively suppress the aromatics-based cycle, resulting in unchanged selectivities to ethene and higher olefins (C₃+). Within the C₃+ fraction, propene selectivity decreases and the selectivity to butenes is enhanced with increasing concentration of the co-fed olefin. Due to the relatively fast methylation rate of C₃–C₆ olefins, the same product distribution at 100% methanol conversion and an identical impact were observed when co-feeding C₃–C₆ olefins.

The present work provides insights into the practical MTO(P) applications, such as Lurgi's MTP process [6–9,38]. In this process, Methanol/DME is introduced to the HZSM-5 catalyst bed loaded in an adiabatic fix-bed reactor [9–12]. After fractionalization of the reactor effluent, the alkene products other than propene, such as C₂= and C₄–C₆ aliphatics, are recycled for further conversion to maximize propene production [9–12,41]. Globally, this process converts about 65% carbon to propene, balanced by LNG and gasoline (mainly aromatics).

Based on the results shown here, the MTP process has a great potential to be tuned from maximum propene production into producing both ethene and propene to meet the fluctuating market demands. Conceptually, this could be achieved through selective recycling of the on-site produced aromatic by-products without changing the reactor configuration or the catalyst. One should note, however, that this approach also promotes to some degree the formation of undesired methane.

On the other hand, adding C₄–C₆ olefins leads to the product distribution independent of the nature of olefinic co-feeds. This indicates that a more fractionated recycling of olefins would not

intrinsically change the olefin concentration produced by methanol. Recycling of the higher olefin fraction with methanol yields, however, more propene than the single pass methanol conversion, because the majority of the carbon in the recycle reacts and is re-distributed into propene through fast olefin methylation and cracking.

Acknowledgments

The financial support from Clariant Produkte (Deutschland) GmbH and fruitful discussion within the framework of MuniCat is gratefully acknowledged.

Appendix A. Supplementary material

Supplementary data associated with this article can be found, in the online version, at <http://dx.doi.org/10.1016/j.jcat.2014.03.013>.

References

- [1] C.D. Chang, Catal. Rev. – Sci. Eng. 25 (1983) 1.
- [2] M. Stöcker, Microporous Mesoporous Mater. 29 (1999) 3.
- [3] T. Mokrani, M. Scurrell, Catal. Rev. – Sci. Eng. 51 (2009) 1.
- [4] U. Olsbye, S. Svelle, M. Bjørgen, P. Beato, T.V.W. Janssens, F. Joesen, S. Bordiga, Angew. Chem., Int. Ed. 51 (2012) 5810.
- [5] K. Hemelsoet, J. Van der Mynsbrugge, K. De Wispelaere, M. Waroquier, V. Van Speybroeck, ChemPhysChem 14 (2013) 1526.
- [6] S. Ilias, A. Bhan, ACS Catal. 3 (2013) 18.
- [7] S. Yurchak, Stud. Surf. Sci. Catal. 36 (1988) 251.
- [8] C.D. Chang, Catal. Today 13 (1992) 103.
- [9] H. Koempel, W. Liebner, Stud. Surf. Sci. Catal. 167 (2007) 261.
- [10] H. Bach, L. Brehm, S. Jensen, 2004, EP 2004/018089 A1.
- [11] G. Birke, H. Koempel, W. Liebner, H. Bach, 2006, EP2006048184.
- [12] M. Rothaemel, U. Finck, T. Renner, 2006, EP 2006/136433 A1.
- [13] B.V. Vora, T.L. Marker, P.T. Barger, H.R. Nielsen, S. Kvisle, T. Fuglerud, Stud. Surf. Sci. Catal. 107 (1997) 87.
- [14] Chem. Eng. News 83 (50) (2005) 18.
- [15] J. Liang, H. Li, S. Zhao, W. Guo, R. Wang, M. Ying, Appl. Catal. 64 (1990) 31.
- [16] C.D. Chang, A.J. Silvestri, J. Catal. 47 (1977) 249.
- [17] I.M. Dahl, S. Kolboe, Catal. Lett. 20 (1993) 329.
- [18] I.M. Dahl, S. Kolboe, J. Catal. 149 (1994) 458.
- [19] I.M. Dahl, S. Kolboe, J. Catal. 161 (1996) 304.
- [20] J.F. Haw, W. Song, D.M. Marcus, J.B. Nicholas, Acc. Chem. Res. 36 (2003) 317.
- [21] U. Olsbye, M. Bjørgen, S. Svelle, K.P. Lillerud, S. Kolboe, Catal. Today 106 (2005) 108.
- [22] W. Song, D.M. Marcus, H. Fu, J.O. Ehresmann, J.F. Haw, J. Am. Chem. Soc. 124 (2002) 3844.
- [23] J.F. Haw, J.B. Nicholas, W. Song, F. Deng, Z. Wang, T. Xu, C.S. Heneghan, J. Am. Chem. Soc. 122 (2000) 4763.
- [24] S. Svelle, F. Joensen, J. Nerlov, U. Olsbye, K.P. Lillerud, S. Kolboe, M. Bjørgen, J. Am. Chem. Soc. 128 (2006) 14770.
- [25] M. Bjørgen, S. Svelle, F. Joensen, J. Nerlov, S. Kolboe, F. Bonino, L. Palumbo, S. Bordiga, U. Olsbye, J. Catal. 248 (2007) 195.
- [26] Z.-M. Cui, Q. Liu, S.-W. Bain, Z. Ma, W.-G. Song, J. Phys. Chem. C 112 (2008) 2685.
- [27] Z.-M. Cui, Q. Liu, Z. Ma, S.-W. Bain, W.-G. Song, J. Catal. 258 (2008) 83.
- [28] S. Teketel, S. Svelle, K.P. Lillerud, U. Olsbye, ChemCatChem 1 (2009) 78.
- [29] S. Teketel, U. Olsbye, K.P. Lillerud, P. Beato, S. Svelle, Microporous Mesoporous Mater. 136 (2010) 33.
- [30] J. Li, Y. Wei, Y. Qi, P. Tian, B. Li, Y. He, F. Chang, X. Sun, Z. Liu, Catal. Today 164 (2011) 288.
- [31] J. Li, Y. Wei, G. Liu, Y. Qi, P. Tian, B. Li, Y. He, Z. Liu, Catal. Today 171 (2011) 221.
- [32] T. Mole, G. Bett, D. Seddon, J. Catal. 84 (1983) 435.
- [33] B.E. Langner, Appl. Catal. 2 (1982) 289.
- [34] M.M. Wu, W.W. Kaeding, J. Catal. 88 (1984) 478.
- [35] L.M. Tau, A.W. Fort, S. Bao, B.H. Davis, Fuel Process. Technol. 26 (1990) 209.
- [36] S. Svelle, P.O. Rønning, S. Kolboe, J. Catal. 224 (2004) 115.
- [37] L.-M. Tau, B.H. Davis, Energy Fuels 7 (1993) 249.
- [38] S. Svelle, P.O. Rønning, U. Olsbye, S. Kolboe, J. Catal. 234 (2005) 385.
- [39] T. Behrsing, T. Mole, P. Smart, R.J. Western, J. Catal. 102 (1986) 151.
- [40] S. Ilias, A. Bhan, J. Catal. 290 (2012) 186.
- [41] W. Wu, W. Guo, W. Xiao, M. Luo, Chem. Eng. Sci. 66 (2011) 4722.
- [42] L.H. Ong, M. Domok, R. Olindo, A.C. van Veen, J.A. Lercher, Microporous Mesoporous Mater. 164 (2012) 9.
- [43] N.Y. Chen, W.J. Reagan, J. Catal. 59 (1979) 123.
- [44] R.M. Dessau, J. Catal. 99 (1986) 111.
- [45] R.M. Dessau, R.B. LaPierre, J. Catal. 78 (1982) 136.
- [46] O. Mikkelsen, P.O. Rønning, S. Kolboe, Microporous Mesoporous Mater. 40 (2000) 95.